On interactions in binary mixtures used in solvent extraction: Insights from combined Isothermal Titration Calorimetry experiments and Molecular Dynamics simulations

Mathilde Coquil, Nathalie Boubals, Magali Duvail, Marie-Christine Charbonnel, Jean-François Dufrêche

Version of Record: https://www.sciencedirect.com/science/article/pii/S0167732221017098
Manuscript_42b174dc2711178a52818b2838fe5ca1

On interactions in binary mixtures used in solvent extraction: Insights from combined Isothermal Titration Calorimetry experiments and Molecular Dynamics simulations

Mathilde Coquil[a], Nathalie Boubals[a], Magali Duvail[b], Marie-Christine Charbonnel[a], Jean-François Dufrêche[b,*]

[a] *CEA, DES, ISEC, DMRC, Univ Montpellier, F-30207 Bagnols-sur-Cèze*
[b] *ICSM, Univ Montpellier, CEA, CNRS, ENSCM, Marcoule, France*

Abstract

Despite its importance, the description of liquid-liquid extraction is made difficult because the link between the experimental methods and the interactions present in the solution is not direct due to the many organisation phenomena that can occur. We propose a new methodology combining microcalorimetric measurements and molecular modelling to better describe the nature and strength of these interactions in these complex fluids by focusing on extractant-diluent mixtures (N,N-dialkylamides+*n*-alkanes). Enthalpies of dilution were obtained by microcalorimetric measurements at 298 K for each *n*-dodecane and *n*-heptane with DEH*i*BA and for *n*-dodecane with DEHBA. These results have been compared, thanks to a new method that we present here, to molecular dynamics simulations carried out on these same systems. We especially analyzed the influence of the alkyl branching of the extracting molecules and the role of the diluent. Globally, the excess enthalpy is such that these mixtures are energetically not very different from regular solutions but the detailed balance shows an important attraction between the extractants, which can lead to the formation of macromolecular entities favouring extraction. Calorimetry appears to be a method of choice for linking experiments and molecular modelling in

*Corresponding author
Email address: jean-francois.dufreche@icsm.fr (Jean-François Dufrêche)

these complex liquid mixtures, and experimental developments could benefit from using it more often, especially to validate force-fields.

Keywords: isothermal titration calorimetry (ITC), molecular dynamics, solution thermodynamics, binary mixtures, dilution

---

1. Introduction

Nuclear energy is a sustainable way of producing low-carbon energy [1] if it is fuel-efficient. The nuclear power cycle can thus use numerous separation processes to optimise and save resources and to limit the volume and lifetime of waste. To this end, numerous separation stages are implemented in the cycle processes, very often with, as in the PUREX process, a solvent extraction stage. The elements in the used nuclear fuel cover the entire periodic table: actinides, lanthanides, metallic precipitates (metaloids, alkalis, alkaline earths, transition metals and poor metals), gases and volatile fission products (noble gases, halogens, etc...) [2].

In order to develop new extraction systems for actinides and lanthanides, many theoretical methods, such as molecular dynamics [3, 4, 5, 6, 7, 8, 9] and DFT [3, 10, 11, 12, 13, 14, 15, 16], have been coupled with experimental studies (X-ray scattering techniques : Small Angle X-ray Scattering SAXS [17, 5, 6], *Small Angle Neutron Scattering SANS* [15], *Small Wide-angle X-ray scattering* SWAXS [18, 8, 9], *Extended X-Ray Absorption Fine Structure* EXAFS [5, 11, 6, 13, 14, 12, 15, 16], *Electrospray Ionization Mass Spectrometry* ESI-MS [4, 10, 9, 15, 16], UV-visible [3, 11, 9], NMR[3, 6], IR [9, 15], *Vapor pressure osmometry* VPO [9], *Time-Resolved Laser-Induced Fluorescence* TRLIF [4]) in the last decades to give a description of aqueous and organic systems, from the atomic to the mesoscopic scale. Some of these studies are interested in isothermal titration calorimetry (ITC) or Van't Hoff's method to determine the thermodynamic quantities of U(VI) [9] extraction and complexation quantities and both potentiometry [16] and UV-visible spectrophotometry [3] to determine the stability constants of the complexes ($\log\beta$). Other studies, strictly experi-

mental, allowed the determination of the thermodynamic extraction quantities of the cations Am(III), Cm(III) and Eu(III) by evaluating the distribution coefficients (DM) at different temperatures by applying the Van't Hoff equation [19], the complexation quantities of U(IV) in the aqueous phase : i) with nitrates by UV-Visible and microcalorimetry [20] and ii) with IDA and ODA ligands by potentiometry and ITC and their structural properties by EXAFS and NMR [21]. Despite recent studies coupling theoretical and thermodynamic studies in the field of recycling chemistry, these theoretical studies do not propose to compare the energy obtained directly by ITC measurements with that obtained from molecular dynamics calculations for liquid-liquid extraction. The comparison of these thermodynamic quantities is therefore at the center of our preoccupations for the development of processes and the improvement of knowledge.

Currently, the industrial process of liquid-liquid extraction PUREX (Plutonium uranium reduction extraction) allows the selective separation of uranium (VI) and plutonium dissolved in nitric acid by TBP (Tributylphosphate) diluted in kerosene [22]. N,N-dialkylamides (monoamides) were proposed as early in 1960's as potential extractants of these actinides to replace TBP [23, 24, 25, 26, 11, 9, 27, 28, 29, 30, 31] and are currently being studied within the framework of the development of the GANEX process, consisting of a grouped separation of the transuranic elements [32]. Their ability to extract hexavalent americium has also been demonstrated [33]. Their use could reduce waste and avoid the oxidation-reduction steps used to separate uranium from plutonium. The molecular structure of these extractants and the acidity of the medium influence the U(VI)/Pu(IV) selectivity [26].

In order to explain the variations in selectivity, the comparison of the thermodynamic extraction of the cations U(VI) and Pu(IV) is interesting. They are a sum of different contributions and $\Delta_{\text{ext}}H$ is obtained from microcalorimetry after correction of the raw data by the thermal effects of cation dilution and solvent-extractant interactions [34, 35]. The specificity of the study of extraction by ITC is the successive addition of small volumes of solvent (diluent + extractant molecule) to the biphasic system, which leads on the one hand to

a phenomenon of dilution mixing of the organic phase and on the other hand to a phenomenon of extraction of uranyl nitrate from the aqueous phase to the organic phase, inducing the formation of a complex in the organic phase with the extractant molecule. This extraction phenomenon induces, respectively, a decrease and an increase in the uranyl concentration, respectively in the aqueous phase and the organic phase, making it possible to identify, on either side of the liquid-liquid interface, the evolution of the heat of solvation of uranyl nitrate.

Many experimental studies and molecular dynamics simulations, to determine the properties of extractant systems containing TBP [36, 37, 38, 39, 40] have been carried out over the last decades and have allowed to understand and predict the thermodynamic, physico-chemical and structural properties of aqueous and organic phases as a function of electrolyte concentration, temperature, acidity of the medium, thus allowing the implementation of extraction process simulation tools such as the PAREX [41] code to facilitate the start-up of production facilities and the design of new processes.

The study of extraction has so far mainly been carried out by complementary experiments and simulations, but this work is all the more difficult as molecular modelling requires precise and robust force fields in order to be successfully implemented. However, thermodynamic and structural quantities only indirectly reflect these interactions, due to the entropic effects that are always important in these aggregated systems. The verification of the molecular model is therefore always done a posteriori. Nevertheless, we believe that there is an experimental quantity which more directly reflects the interactions: it is the enthalpy H (or the internal energy E which is practically equivalent for the condensed phases). H (or E) are indeed only statistical averages of interaction energies. This quantity can be measured by calorimetry experiments (such as ITC) and direct comparisons can then be obtained. *It is such a work that we propose to present for the first time in this article in the case of mixtures between extractant and diluent.* This work is all the more important as the comparison here is direct since the enthalpy can be calculated directly in a single molecular simulation contrary to entropy or Gibbs energy which require several simulations

and a thermodynamic integration process to be evaluated correctly.

The liquid-liquid extraction of actinides is a succession of mechanisms taking place in the aqueous phase, at the interface and in the organic phase. Ions are dehydrated ($\Delta_{\text{deshyd}}H$) then the cation and its counter-ion are transferred from the aqueous phase to the organic phase corresponding to a change in solvation ($\Delta_{\text{tr}}H$) and are finally complexed in the organic phase with the extractant ($\Delta_{\text{compl}}H$). The phenomenon of transfer and change of solvation has been relatively well studied in the literature for many electrolytes and corresponds to the difference between the enthalpies of hydration, but since the lattice energies - allowing to quantify the forces between the ions in an ionic solid - are identical, on both sides of the interface, this comes down to examining the difference between the enthalpies of dissolution [42]. The enthalpy of solvation of an ion is the succession of two mechanisms, the first corresponds to the solute-solvent interaction (ligation) and the second to the dispersion due to the reorganization of the solvent around the solute and water molecules in the first sphere of solvation [43, 44, 45]. It is possible to follow the variation in the enthalpy of dissolution of uranyl nitrate by considering the different phases, aqueous and organic, with different compositions, separately.

For the uranyl ion, several studies have explored the hydration properties of the ion in aqueous solution and its organization in organic phase with ligands. The structural properties can be determined by the study of radial distribution functions (RDF). In the aqueous phase, it was shown that the cation was surrounded by two oxygen atoms at an equilibrium distance U-O_U of 1.75 to 1.78 Å and surrounded by five water molecules in the first hydration sphere in an equatorial plane for a distance U-O_W of 2.41 to 2.44 Å [14, 46, 47, 48]. In the organic phase, the organization with different monoamides ~~(DEHiBA, DEHBA, DEHDMBA)~~ (N,N-di(2-ethylhexyl)*iso*butyramide (DEH*i*BA), N,N-di(2-ethylhexyl)*n*-butyramide (DEHBA), N,N-di(2-ethylhexyl)dimethylbutyramide (DEHDMBA) by crystallography [12] and at different concentrations of DEH*i*BA (0.5 mol/L and 1.5 mol/L) [9] was studied. A new polarizable force field has recently been developed which allows to reproduce the experimental structural

properties of the ion in both aqueous and organic phase [46]. It seems essential to complement these structural studies with thermodynamic studies. To do this, several possibilities, with different objectives, can be used to calculate the enthalpy of the multicomponent mixture at different concentrations and deduce the enthalpy of dissolution or, as Grossfield *et al.* did for the chloride ion, to calculate the enthalpy of hydration for clusters containing from one to six molecules of water with a single ion [49].

The extraction of uranyl nitrate from a $LiNO_3$ medium by the extracting molecule DEH*i*BA diluted in *n*-dodecane is especially interesting, because it is a molecule selected to extract uranium (VI) during the first stage of the GANEX process [32]. The complex thus formed is mainly $UO_2(NO_3)_2$DEH*i*BA_2. The $LiNO_3$ medium allows, in a first time, to free itself from the extraction of nitric acid that can induce the formation of different complexes, such as for example trinato complexes containing protonated ligands in the external sphere of coordination of cation [50, 11]. To determine the enthalpy of dissolution of uranyl nitrate experimentally, the salt in crystalline, non-hexahydrated form should be added to a solution of $LiNO_3$ 3M and the change in enthalpy measured during a succession of salt additions. In the organic phase, uranyl nitrate, being present in complexed form with DEH*i*BA, the experiment would be all the more complicated as the complex would be destabilized. In view of these experimental difficulties, it seems more practical to implement the opposite process, which is dilution. We have therefore chosen the enthalpies of dilution to validate our molecular dynamics calculations. From these enthalpies, we will be able to estimate the enthalpies of solution of the different solutes in each phase and estimate the energy of solvation change. The enthalpy of dilution as well as the enthalpy of solution (dissolution) can be related to the enthalpy of excess. Previous work has led to the development of a thermodynamic model for electrolyte-free mixtures [51]. What we propose is simpler and can be applied to all binary mixtures, but also to multicomponent mixtures, and will allow us to link our experiments for liquid-liquid extraction and separate studies of aqueous and organic phases by ITC to our simulations of molecular dynamics.

This study focused on the evolution of the enthalpy of the organic phase not charged with uranium thus presents several interests and allows to evaluate the molecular interactions within mixtures (N,N-dialkylamides+n-alkanes) with linear and branching alkyl chains: (i) to develop a methodology on simple binary mixtures, (ii) to validate our methodology by showing that intermolecular interactions make it possible to determine the enthalpy of dilution and the parameters of the corresponding force field, and (iii) to obtain the enthalpy of dilution of the organic phase to deduce it from the heat measured experimentally during the study of a biphasic system by ITC.

As far as we know, in the past, only excess enthalpies on mixtures containing short chain length monoamides [52] are available in the literature. Furthermore, similar studies of calorimetry and/or molecular dynamics simulation experiments have been carried out on other binary mixtures but they only give the enthalpies of excess and they do not highlight the link between the different enthalpies (mixture, excess and dilution). Mixtures with n-alkanes have been relatively well studied in the literature because of their apparent simplicity and their use as a diluent for extracting molecules in nuclear fuel reprocessing, however most studies on these systems focus on excess enthalpies. This is the case in particular for mixtures (diluent + extractant) containing oxygenated donors (phosphoryl-oxygen) which have been widely studied by experience [37, 36] and by molecular dynamics [38]. Firstly, the increase in the length of the solvent chain was correlated with the increase in the excess enthalpy for a given extractant [36, 38], long chain n-alkanes having greater ease in breaking the dipole-dipole bonds of oxygenated donors. It has also been shown that neutral organophosphorus extractants are self-associating and this behavior explains the endothermicity of the excess enthalpy. Secondly, the influence of the nature of the extractant was studied [37] by comparing the systems ~~(TBP+dodecane) and (DBBP+dodecane)~~ (tri(n-butyl)phosphate (TBP)+n-dodecane) and (di(n-butyl)butylphosphonate (DBBP)+n-dodecane) under the same temperature conditions [36]. It appears that the excess enthalpy of the system (TBP+n-dodecane) is higher than the system (DBBP+n-

dodecane). Schwabe studied [53] a TBP isomer, T*i*BP, with branching chain (isobutyl) on O-P(O), instead a linear *n*-butyl chain. From the results, we have determined that for these extracting molecules diluted in *n*-hexane, the excess enthalpy is about 100 J mol^{-1} higher in favour of mixing with the isobutyl branching. In view of this information, we wondered whether for other *n*-alkane-containing systems we had the same behaviour.

Similar observations were made by Valero and his colleagues in two articles on mixtures (haloalkane+*n*-alkane) [54, 55]. They deduced the same conclusions as for systems containing oxygenated donors regarding the influence of the length of the *n*-alkane chain, except for 1-halogenohexadecane which has the lowest excess enthalpy. They also compared the behaviour of two isomers in *n*-alkanes: terbutylchloride and 1-chlorobutane and they found that the excess enthalpy of the systems (terbutylchloride+*n*-alkane) was still higher than the systems (1-chlorobutane+*n*-alkane) for the same number of carbon atoms of the diluent. According to the authors, this would be due both to the existence of molecular orientation correlations within the *n*-alkane family - all the more important because the carbon number of the *n*-alkane is important - and to the fact that terbutylchloride is a globular molecule compared to 1-chlorobutane and would thus have a greater effectiveness in disordering the linear molecules of *n*-alkanes. TiBP being a more globular molecule than TBP, it can therefore be hypothesized that its behaviour when mixed with alkanes is similar to terbutylchloride. About the organization within *n*-alkane molecules, Bothorel et al. [56] experimentally constructed isothermal depolarized intensity diagrams of several *n*-alkanes with cyclohexane and carbon tetrachloride and found that the solutions of (*n*-pentane+cyclohexane), (*n*-pentane+carbontetrachloride) and (*n*-hexane+cyclohexane) were ideal. This would be due to the fact that short-chain *n*-alkanes have a low anisotropy and have little molecular orientation compared to longer-chain *n*-alkanes, which are placed parallel to each other. Knowing that in an ideal solution, the interactions between molecules of different species and of the same species are identical, this would be due to identical molecular correlations for each species in solution.

Other mixtures (trialkylamine + aliphatic hydrocarbon) containing donor nitrogen atoms were studied [57]. The excess enthalpies of these mixtures are endothermic. In all binary systems studied, it seems obvious that the asymmetry of the enthalpy of excess is due to a significant difference between the molar volumes of the components of the mixture and that the maximum is moved to the side of the mixture with the lowest molar volume. This asymmetry was also reported by Fenby et al. [58]. To explain the sign of the excess enthalpy, Fenby considers it to be the sum of different interactions. A first physical interaction induces a positive contribution and a second chemical interaction (complex formation) induces a negative contribution. Mixture data (monoamides+hydrocarbons) were found but only for short linear chain monoamides [52]. The excess enthalpy is endothermic for the monoamides DEA (N,N-diethylacetamide) and DMA (N,N-dimethylacetamide) in mixture with *n*-hexane. This study was motivates by the lack of data on monoamides of interest used in the reprocessing of nuclear fuel.

The manuscript is organised as follows. First the methodology to measure and calculate dilution enthalpy is presented. In the second part, the experimental and molecular dynamics methods are described. Results are presented and discussed in the last section for the systems (*n*-dodecane + DEH*i*BA), (*n*-dodecane + DEHBA) and (*n*-heptane + DEH*i*BA). These mixtures are reference solution for the GANEX process [32] which can be used for the reprocessing of spent nuclear fuels.

2. Theory

2.1. Expression of dilution enthalpy

Let consider two compounds **1** and **2** corresponding respectively to the solute and the solvent. A dilution process consists in transferring a pure solvent into a solution phase containing the solute. The total amounts of matter do not change in the system, but the amounts of solvent diminish in the solvent phase and increase in the solution. The dilution process takes place in a closed system.

Thus, the pressure is imposed and the temperature is constant. The system only exchanges energy with the outside environment. Small amounts of pure compound **2** are added gradually implying thus the increase of the solvent molar fraction x_2 and the decrease of the solute molar fraction x_1 in the binary mixture. The dilution of n-alkane **2** in a solution containing the solute **2** can be described as follows

$$\underset{\text{pure}}{2}\ ^{*} \longrightarrow \underset{\text{in mixture with 1}}{2} \tag{1}$$

Dilution is a physical process. In the microcalorimetry experiments, the pure diluent is added by successive additions of very small amounts of diluent Δn (typically 10 µL) compared to the initial amount (typically 1 mL). Thus, the measured enthalpy variation corresponds to the partial molar enthalpy in the mixture minus the reference initial term (pure diluent). The enthalpy of dilution $\Delta_{\text{dil}}H$ is therefore

$$\Delta_{\text{dil}}H = h_2 - h_2^* \tag{2}$$

where h_2 is the partial molar enthalpy of n-alkane in the mixture, h_2^* is the molar enthalpy of pure n-alkane and x the molar fraction of compound **1** ($x = x_1$).

The molar enthalpy of the mixture h is

$$h(x) = \sum_{i=1}^{z} x_i h_i \tag{3}$$

where x_i is the molar fraction of the compound i and h_i the partial molar enthalpy of i.

The partial molar enthalpy of the solvent can be expressed as a function of the molar enthalpy of the mixture. Considering that h is the function defined by $h(x_1)$, then the enthalpy of the H mixture

$$H = (n_1 + n_2)h(x) = (n_1 + n_2)h(\frac{n_1}{n_1 + n_2}) \tag{4}$$

The partial molar enthalpy of n-alkane is

$$h_2(x) = \frac{\partial H(x_1)}{\partial n_2} \tag{5}$$

$$h_2(x) = \frac{\partial[(n_1+n_2)h(\frac{n_1}{n_1+n_2})]}{\partial n_2} \tag{6}$$

$$h_2(x) = [h(\frac{n_1}{n_1+n_2}) + (n_1+n_2)\frac{-n_1}{(n_1+n_2)^2}h'(\frac{n_1}{n_1+n_2})] \tag{7}$$

$$h_2(x) = h(x_1) - \frac{n_1}{(n_1+n_2)}h'(x) \tag{8}$$

Finally, the partial molar enthalpy of n-alkane is

$$h_2(x) = h(x) - x\frac{\partial h(x)}{\partial x} \tag{9}$$

Thus, it can be possible to express $\Delta_{\text{dil}}H(x)$ as a function of the molar enthalpy of the mixture. The enthalpy of dilution $\Delta_{\text{dil}}H(x)$ is

$$\Delta_{\text{dil}}H(x) = h(x) - x\frac{\partial h(x)}{\partial x} - h_2^* \tag{10}$$

The molar enthalpy of excess h^{E} is the difference between the enthalpy of the real mixture h and the enthalpy of ideal mixture in the same conditions of pressure and temperature

$$h^{\text{E}}(x) = h - \sum_{i=1}^{z} x_i h_i^* \tag{11}$$

where h_i^* is the molar enthalpy of the pure constituent i. For a binary mixture, it reads

$$h(x) = h^{\text{E}} + [xh_1^* + (1-x)h_2^*] \tag{12}$$

If we replace h in Eq. 10 by its expression given in Eq. 12 we obtain

$$\Delta_{\text{dil}}H(x) = h^{\text{E}}(x) - x\frac{\partial h^{\text{E}}(x)}{\partial x} \tag{13}$$

2.2. Data treatment

According to the Euler's theorem, the molar enthalpy of mixture has two limits

$$\lim_{x\to 0} h(x) = h_2^*, \tag{14}$$

$$\lim_{x \to 1} h(x) = h_1^*. \tag{15}$$

Therefore, according to the definition of the enthalpy of excess, we have

$$\lim_{x \to 0} h^{\mathrm{E}}(x) = 0, \tag{16}$$

$$\lim_{x \to 1} h^{\mathrm{E}}(x) = 0. \tag{17}$$

With respect to these conditions, Redlich and Kister [59] proposed series of polynomials to represent all excess quantities. Thus, for the enthalpy of excess it is possible to write

$$h^{\mathrm{E}}(x) = x(1-x) \sum_{\mathrm{k}=0}^{n} a_k (2x-1)^k \tag{18}$$

where a_k and k are adjustable parameters.

The enthalpy of the mixture is obtained by introducing the expression of the excess enthalpy (Eq. 18) into the expression giving the molar enthalpy (Eq. 12). So, it reads

$$h(x) = x(1-x) \sum_{\mathrm{k}=0}^{n} a_k (2x-1)^k + [x h_1^* + (1-x) h_2^*] \tag{19}$$

where h_1^* and h_2^* are adjustable parameters.

The enthalpy of dilution, as for $h(x)$ and $h^{\mathrm{E}}(x)$, can be expressed in a polynomial form. The procedure consists in deriving $h^{\mathrm{E}}(x)$ (Eq. 18) and determining the expression of $\Delta_{\mathrm{dil}} H(x)$ according to Eq. 13. Therefore, we obtain

$$\Delta_{\mathrm{dil}} H(x) = x^2 \sum_{\mathrm{k}=0}^{n} a_k (2x-1)^k - (2x^2 - 2x^3) \sum_{\mathrm{k}=0}^{n} a_k k (2x-1)^{k-1} \tag{20}$$

The challenge here is to find a method that consists in determining any quantity from the known data. Indeed, through experiments and simulations we do not always have the same thermodynamic quantities available. Dilution experiments measure the heat of dilution $\Delta_{\mathrm{dil}} H(x)$ whereas molecular dynamics simulation calculate the enthalpy of the mixture $h(x)$. We will therefore study two possible cases, the first is the one where only the dilution enthalpy $\Delta_{\mathrm{dil}} H(x)$ is available, and the second case is the one where the molar enthalpy $h(x)$ is available.

2.2.1. Enthalpy of dilution known

When $\Delta_{\text{dil}}H(x)$ is the known data, two approaches are available to determine $h^{\text{E}}(x)$: (i) solving the differential equation (Eq. 13), or (ii) approximating the solution of the differential equation. The molar enthalpy of the mixture can then only be approximated by combining simulations and experiments.

In the case of solving the differential equation (Eq.13), which is a first order linear differential equation, the variation of the constant is used to find the solution $h^{\text{E}}(x)$. We obtain

$$h^{\text{E}}(x) = x \int_x^1 \frac{\Delta_{\text{dil}}H(x)}{x^2} dx \tag{21}$$

Considering measurements made only in the interval $I = [x_{\text{min}}; x_{\text{max}}]$ the integral is not defined for $x = 0$. Decomposing Eq. 21, it comes

$$h^{\text{E}}(x) = x \int_x^{x_{min}} \frac{\Delta_{\text{dil}}H(x)}{x^2} + x \int_{x_{min}}^{x_{max}} \frac{\Delta_{\text{dil}}H(x)}{x^2} + x \int_{x_{max}}^1 \frac{\Delta_{\text{dil}}H(x)}{x^2} dx \tag{22}$$

In the case of approximating solution of the Eq. 13, the data have been adjusted by nonlinear regression (Eq. 20) with $n = 0, 1, 2, 3$ and 4. For the best fit, $h^{\text{E}}(x)$ is then calculated with the same parameters a_k as $\Delta_{\text{dil}}H(x)$.

2.2.2. Molar enthalpy known

In that case, the enthalpy of the mixture $h(x)$ have been adjusted by equation 19 for $n = 0, 1, 2, 3$ and 4. The excess enthalpy $h^{\text{E}}(x)$ and dilution enthalpy $\Delta_{\text{dil}}H(x)$ are calculated with the same parameters a_k using Eq. 18 and Eq. 20.

3. Materials and methods

3.1. Chemical products

~~*n*-dodecane and *n*-heptane were purchased from Sigma Aldrich. DEHBA and DEHiBA were synthesized~~

n-dodecane and *n*-heptane were purchased from Sigma Aldrich, with analytical grade (purity > 99 %). The molecules DEHBA and DEH*i*BA were

synthesized by Pharmasynthese (Lisses, France), with purity 98 % and 99 %. The molecules were used without further purification and the concentration of mother solutions amide-alkane were checked by a classical non aqueous titration (with $HClO_4$ in acetic medium).

3.2. Microcalorimetry experiments

Microcalorimetric measurements were performed at 25 °C using a Thermal Activity Monitor (TAM 2277) microcalorimetric system (Thermometric TA Instruments). This device is based on a precise thermostated water bath (± 0.1 mK per 24 h) which acts as a heat sink and can hold up to four independent calorimetric units. A ligand solution (n-alkane+monoamide) or in some cases pure monoamide was introduced in the calorimeter thanks to a 1 mL glass cell and a solvent was added into the cell through a fine gold cannula. The solution in the cell was stirred with a gold propeller. The volume of titrant was injected with a programmable motor-driven Thermometric Lund pump equipped with a 500 μL Hamilton syringe. Each calorimetric experiment was performed at least twice (Fig. 1).

The raw data obtained are shown in the figure SI.1 on Supporting Information. Each peak represented on the curve results from injections of the solvent into the cell. The integration of the power peaks allows the heat of reaction Q_P to be obtained and were converted to enthalpy according to

$$\Delta H = \frac{Q_P}{\Delta n} \tag{23}$$

The temperature in the cell during a dilution experiment (some hours) is considered as better as 10^{-3} °C. The response of the equipment (heat measured) was checked with a classical well-known reaction (dilution of propanol-1 10 % in H_2O) [60] with values obtained better than +/-2 %. The uncertainties of dilution enthalpy obtained from twice experiments at least is then better than 10 %.

3.3. Molecular Dynamics simulations

3.3.1. Simulations method

Molecular dynamics simulations of pure n-alkanes (n-heptane and n-dodecane) and monoamides (DEHiBA and DEHBA) at different molar fractions (monoamides x_1 + alkanes x_2) have been carried out in the NPT ensemble with SANDER14, a module of AMBER14 [61] using explicit polarization. The Andersen thermostat [62] and the Berendsen barostat [63] have been used respectively to maintain the temperature at 298.15 K and the pressure at 1 bar. The systems were equilibrated in two steps : first, the systems have been heated at 500.15 K in order to homogenize the molecules and then they have been cooled down to 298.15 K for about 2 ns. Then, production runs have be collected for 3 ns. Periodic boundary conditions were applied to the simulation boxes. Long-range interactions have been calculated using the particle-mesh Ewald method [64]. The non-bonded interaction cutoff is 15 Å. VMD was used to make the MD simulations snapshots [65]. The simulations boxes were built with PACKMOL [66]. The number of molecules of n-alkanes was kept constant in the molar fraction range [0; 0.5] and the number of extractant molecules was kept constant in the molar fraction range [0.5; 1]. The compositions and the densities of the binary mixtures (n-dodecane + DEHiBA),(n-dodecane + DEHiBA) and (n-heptane + DEHiBA) are presented in Table 1 and they are labelled as mixtures A, B and C respectively.

The n-heptane and n-dodecane are described by the force field we recently developed [67] and it is based on the one developed by Siu and al.[68] for long hydrocarbons chains.

Table 1: [a] Monoamide molar fraction, [b] Number of monoamide molecules, [c] Number of *n*-alkane molecules, [d] density of the mixture and [e] fluctuation of the density. The indexes A, B and C identify the mixtures: A (*n*-dodecane + DEH*i*BA), B (*n*-dodecane + DEHBA) and C (*n*-heptane + DEH*i*BA)

[a]x_1	[b]N_1	[c]N_2	[d]d_A	[e]Δd_A	[d]d_B	[e]Δd_B	[d]d_C	[e]Δd_C
0	0	750	0.749	2.03E-03	0.749	2.03E-03	0.676	2.79E-03
0.10	83	750	0.763	1.81E-03	0.764	1.94E-03	0.716	2.35E-03
0.20	188	750	0.777	1.58E-03	0.778	1.66E-03	0.747	2.31E-03
0.30	322	750	0.790	1.62E-03	0.791	1.57E-03	0.771	1.92E-03
0.40	500	750	0.802	1.42E-03	0.803	1.26E-03	0.791	1.73E-03
0.50	750	750	0.811	1.22E-03	0.813	1.36E-03	0.807	1.41E-03
0.60	750	500	0.823	1.22E-03	0.824	1.27E-03	0.820	1.58E-03
0.70	750	322	0.832	1.29E-03	0.833	1.33E-03	0.832	1.56E-03
0.80	750	188	0.839	1.38E-03	0.840	1.11E-03	0.840	1.82E-03
0.90	750	83	0.848	2.14E-03	0.850	1.50E-03	0.848	2.54E-03
1	750	0	0.854	2.55E-03	0.855	2.18E-03	0.854	2.55E-03

3.3.2. Data analysis

The total energy is defined by:

$$E_{\text{tot}} = E_{\text{kin}} + E_{\text{pot}} \tag{24}$$

with E_{kin} the kinetic energy of the system and E_{pot} its potential energy, that can be decomposed as follows

$$E_{\text{pot}} = E_{\text{inter}} + E_{\text{intra}} \tag{25}$$

where E_{inter} is the intermolecular energy and E_{intra} is the intramomolecular energy The intermolecular and intramolecular energy can be decomposed as follows

$$E_{\text{inter}} = E_{\text{vdw}} + E_{\text{el}} + E_{\text{pol}}, \tag{26}$$

$$E_{\text{intra}} = E_{\text{bond}} + E_{\text{angles}} + E_{\text{dihedral}} + E_{\text{14vdw}} + E_{\text{14el}}. \tag{27}$$

where E_{vdw} is the van der Waals Energy, E_{el} is the electrostatic energy, ~~E_{Hbond} the energy of hydrogen bonds~~, E_{bond} the bond energy, E_{angles} the angles energy, E_{dihedral} the dihedres energy, E_{14vdw} et E_{14el} respectively the Van der Waals and electrostatic energies between atoms separated by three bonds (the atoms 1 and 4 in the 1-4 chain) and E_{pol} the polarizable energy. The intramolecular energy is part of the potential energy

$$E_{\text{intra}} = E_{\text{bond}} + E_{\text{angles}} + E_{\text{dihedres}} + E_{\text{14vdw}} + E_{\text{14el}} \tag{28}$$

Particular attention has been accorded to the accuracy of the thermodynamic properties of water with different models [69, 70]. An underestimation of water entropy of 20 % for the translational contribution and 40 % for the rotational contribution is reported by Pascal [69]. After quantum corrections, the entropy and calorific capacity values obtained are closed to experimental data. Vega *et al.* [70] only make a correction of 3R to the calorific capacity C_{P} which corresponds to the vibrational contribution of the C_{P} of water. The problem come from the fact that considering the vibration frequencies of the molecules, quantum mechanics has to be considered to describe vibrational enthalpy. In fact,

the situation is not that bad because we are only interested an intermolecular forces associated to mixing. We considered that the intramolecular vibrations were independent on the composition so they are assumed to be constant during dilution. Within that approximation, intramolecular terms can be removed for the calculation of the total enthalpy.

The enthalpy for each molar fraction is calculated by:

$$h(x) = E_{\text{tot}}(x) - E_{\text{intra}}(x) + PV(x) \tag{29}$$

4. Results and discussion

4.1. Dilution enthalpy, excess enthalpy and enthalpy of the mixture

The methodology consists of isothermal calorimetric titration experiments on the first part, and molecular dynamics simulations of mixtures and pure bodies over the whole range of molar fractions on the second part. The experimental data directly allow us to obtain the enthalpy of dilution for which we have developed an algebraic representation based on the work of *Redlich and Kister*. The experimental data are therefore adjusted by the equation 20 for $n = 0, 1, 2, 3$. The simulations allow us to obtain the enthalpy of the mixture as a function of the molar fraction of monoamide for which we have added a linear term to the Redlich and Kister excess enthalpy representation [59]. The simulated data are therefore adjusted by the equation 3 for $n = 0, 1, 2, 3$. For all systems, we calculate the mean square deviation between the simulated and experimental data, first only in the experimental measuring range and then in the entire molar fraction range. This allows us to decide which order of polynomial we use for each experiment to calculate the enthalpy of excess. It goes without saying that the more the experimental measurements are extended over the entire molar fraction range, the closer the excess enthalpy we estimate will be to reality. Conversely, this magnitude will be overestimated. We will present this complete method through the study of the system (n-dodecane+DEHiBA).

4.1.1. (n-dodecane + DEHiBA)

As mentioned above, we carried out experiments in order to dilute DEH*i*BA with *n*-dodecane over the entire molar fraction, *i.e.*, from $x_{\mathrm{DEH}i\mathrm{BA}} = 0$ to $x_{\mathrm{DEH}i\mathrm{BA}} = 1$ with a non-constant molar fraction step, and corresponding molecular dynamics simulations with a molar fraction step of $\Delta x_{\mathrm{DEH}i\mathrm{BA}} = 0.1$ (see section 3.3.1 for the protocol and see Table 1 for the composition and density of the simulation boxes).

The dilution enthalpy of mixture (*n*-dodecane + DEH*i*BA) is represented in Figure 3. Experimental data (black squares) are only available between $x_{\min}$ and $x_{\max}$ where $x_{\min} = 0.13$ and $x_{\max} = 0.97$. The raw data has been adjusted using Equation 20 for $n = 2$ (red line). The other curves, obtained from the molecular dynamics simulations, will be described later. Therefore, it is not possible to calculate h^{E} directly using Equation 21. An adjustment of the data was necessary in the intervals where no experimental data could be obtained. The data were estimated by $y_1(x) = ax^2$ ($a = 9.82949$ kJ mol$^-$1) in the interval $I_1 = [0; x_{\min}]$ and by $y_2(x) = ax^2 + bx + c$ ($a = 5.40127$ kJ mol$^-$1, $b = -4.46562$ kJ mol$^-$1 and $c = 2.48854$ kJ mol$^-$1) in the interval $I_2 = [x_{\max}; 1]$ (in fact, only the adjustment in the interval I_2 is necessary to integrate). To estimate the excess enthalpy, two methods were used, *i.e*, (i) the direct method by using the equation 21 and (ii) the indirect method by adjusting the parameters of Equation 20 (with $n = 3$), the parameters for the dilution enthalpy and the excess enthalpy being the same.

The excess enthalpy of mixture (*n*-dodecane + DEH*i*BA) (see figure 4) is endothermic over the entire molar fraction range for (*n*-dodecane + DEH*i*BA) and the maximum is located at $x = 0.42$. The mean square deviation is 1.8 J mol^{-1} for a deviation of 0.2 % from the mean values between the two methods. As for the enthalpy of dilution, the curves obtained from the molecular dynamics simulations, will be described later.

The molecular dynamics raw data are presented in Figure 5. An adjustment of the raw data $h(x)$ using Equation 19 allowed obtaining a continuous molar enthalpy for different n values. The fitted curves of $h(x)$ are presented in the Fig. 5 (respectively the green and blue lines correspond to $n = 1$ and $n = 2$ values). From these fitted curves, we calculated both the excess enthalpy (see Figure 4) and the enthalpy of dilution (see Figure 3) with the same parameters a_k (listed in Table 1 on Supporting Information). For these two enthalpic quantities, the simulated values are close to the experimental values. The mean square deviations calculated between the fitted experimental molar excess enthalpy obtained and the simulated molar excess enthalpy obtained by fitting Redlich-Kister model is respectively 47 J mol^{-1} for $n = 1$ and 48 J mol^{-1} for $n = 2$. In both cases, the deviation is 6.8 % from the mean values. Molecular dynamics calculations allow us to obtain excess enthalpy very close to experimental values. It should be noted that the two dilution enthalpy curves predicted by the two Redlich-Kister equations differ more than the two excess enthalpy curves on which they have been fitted. This comes from the derivation which induces noise in the curves. We show that MD and experiments are consistent, but the precision of MD simulations does not reach the experimental precision because of the accuracy of the simulations. Finally, we estimated the molar enthalpy of the experimental mixture by adding the ideal term calculated by molecular dynamics to the excess enthalpy calculated by adjustment from raw experimental data (red line in Fig. 4). The estimation of the excess enthalpy from the ideal term calculated by molecular dynamics and the excess term calculated by experiment gives good results. The mean square deviations are the same to those of the excess enthalpy. However, the deviation is 0.11 % from the mean values. The adjusted parameters for experimental and simulated data and the mean square deviations between experimental and molecular dynamic simulated data for the (n-dodecane+DEHiBA) mixture are respectively available in Tables 1 and 2 on Supporting Information, respectively.

Table 3 on Supporting Information shows the validation criteria for determining which adjustment of the molecular dynamics data allows the experimental data to be reproduced. The first criteria defined is the limit value of the dilution enthalpy when $x_{\mathrm{DEH}i\mathrm{BA}} = 1$. In this first case, the experimental limit value is closer to the molecular dynamics data for $n = 2$ (35 % $n = 1$ and 1.9 % $n = 2$). The second criteria used is the coordinate $(x_{\mathrm{DEH}i\mathrm{BA}}, \Delta_{\mathrm{dil}}H$ corresponding to the intersection of the dilution enthalpy and the excess enthalpy (when the excess enthalpy is maximum, the derivative is zero). In this case, the experimental coordinates $(x_{\mathrm{DEH}i\mathrm{BA}}, \Delta_{\mathrm{dil}}H)$ are in better agreement with the molecular dynamics data for $n = 1$ (difference of 4.8 % for $x_{\mathrm{DEH}i\mathrm{BA}}$ and 2.5 % for $\Delta_{\mathrm{dil}}H$). Nevertheless, the difference between experimental and molecular dynamics data for $n = 2$ is not very large, only 9.5 % for $x_{\mathrm{DEH}i\mathrm{BA}}$ and 3.9 % for $\Delta_{\mathrm{dil}}H$. In conclusion, to represent the enthalpy of dilution, the adjustment $n = 2$ is more representative of the experimental data and in the case of the excess enthalpy, the adjustment $n = 1$ is the most representative. To compare the systems, we will in any case take the adjustments for $n = 2$ for molecular dynamics simulations.

4.1.2. (n-dodecane + DEHBA)

As already done for the (n-dodecane+DEHiBA) mixtures, we carried out experiments to dilute DEHBA with n-dodecane only over a small range of molar fraction $0.15 < x < 0.33$ and corresponding molecular dynamics simulations with a molar fraction step of $\Delta x_{\mathrm{DEHBA}} = 0.1$ (see section 3.3.1 for the protocol and see Table 1 for the composition and density of the simulation boxes).

Figure 6 shows the enthalpy of dilution as a function of DEHBA molar fraction. The other curve (green curve), obtained from the molecular dynamics simulations, will be described later.

The molecular dynamics raw data are presented in Figure SI.3 on Supporting Information. An adjustment of the raw data $h(x)$ from equation 19 allowed

obtaining a continuous molar enthalpy for different n values. Only one fitted curve of $h(x)$ is presented in the Fig. SI.3 on Supporting Information (the green line correspond to $n = 1$ value). From this fitted curve, we calculated both the excess enthalpy (see Figure 9) and the enthalpy of dilution (see figure 6) with the same parameters a_{k}. The mean square deviation is 10 J mol^{-}1 for a deviation of 2.5 % from the mean values between the available raw experimental and the fitted molecular dynamics enthalpy of dilution (for $n = 1$). The simulations allow us to obtain the enthalpy of the mixture as a function of the molar fraction of monoamide for which we have added a linear term to the *Redlich and Kister* excess enthalpy representation.

We estimated the molar enthalpy of the mixture by experiment and compared it to that calculated by molecular dynamics simulations. To do this, we added the linear term calculated by molecular dynamics to the experimental excess enthalpy calculated with the same parameters a_{k} as for the fitted enthalpy of dilution (red line in Figure 6). The mean square deviation is 1460 J mol^{-}1 for a deviation of 2.3 % from the mean values between the fitted experimental (red line in Fig. SI.3 on Supporting Information) and molecular dynamics (green line in Fig. SI.3 on Supporting Information) enthalpy of dilution (both for $n = 1$). The agreement between these curves is therefore very good. We also calculated the excess enthalpy of mixture (n-dodecane + DEHBA) from molecular dynamics simulations and compared it to the excess enthalpy of mixture (n-dodecane + DEHiBA) (Figure SI.2 on Supporting Information). We have determined that for these extractant molecules diluted in n-dodecane, the excess enthalpy is about 423 J mol^{-}1 higher in favour of mixing with the isobutyl branching (DEHiBA). The excess enthalpy is endothermic over the entire molar fraction range for (n-dodecane + DEHiBA) and the maximum is located at ($x_{\mathrm{DEH}i\mathrm{BA}} =$ 0.4 while for (n-dodecane + DEHBA) it is endothermic up to $x_{\mathrm{DEH}i\mathrm{BA}} = 0.8$ and then changes sign and the maximum is located at $x_{\mathrm{DEHBA}} = 0.29$. We also observed that the excess enthalpies are asymmetric with a maximum shifted towards mixtures with the lowest molar volume. This behaviour has already

been reported by Grauer *et al.* [57] and Fenby *et al.* [58].

4.1.3. (n-heptane + DEHiBA)

We carried out experiments to dilute DEH*i*BA with another *n*-alkane, the *n*-heptane only over a small range of molar fraction $0.15 < x < 0.39$ (due to the volatility of *n*-heptane, experimental measurements could not be made over a large range of molar fractions) and molecular dynamics simulations with two force field : the first was described by Chen *et al.* [71] and the second was described by Sukhbaatar *et al.* [67]. As for the mixture (*n*-dodecane + DEH*i*BA), we estimated the missing data by $y_1(x) = ax^2 + bx$ ($a = 1368.3$, $b = 1139.2$) in the interval $I_1 = [0; x_{min}]$ and by $y_2(x) = a + b\ln(x)$ ($a = 543.13$ and $b = 182.7$) in the interval $I_2 = [x_{min}; 1]$. The experimental enthalpy was then calculated by integration (by equation 19). We used this excess enthalpy to estimate the molar enthalpy of the experimental mixture (see red line in Fig. 8). The agreement with the enthalpy of the simulated mixture is very good (the deviation is 0.73 %). The enthalpy of dilution calculated from the first force field is positive over the entire molar fraction, while that calculated from the second force field changes sign at $x_{\mathrm{DEH}i\mathrm{BA}} = 0.56$ (Figure 7). A concordance of the two force fields can be seen for the lowest molar fractions in DEH*i*BA. The mean square deviation between the experimental data and the simulated data is 12 J mol^{-1} for the first force field and 17 J mol^{-1} for the second force field in the measuring range. In the measurement range we studied, the first force field gives results closer to the experiments than the second force field, but the difference between the two force fields is really significant only beyond the measurement range (see Fig. 7).

4.2. Coordination around extractant molecules

One method for determining whether extractant molecules is self-associated is to calculate the coordination numbers from the integral of the radial distribution function $g(r)$. The C_{carb} carbon atom of the carbonyl function was chosen to characterize the coordination in all mixtures. The RDF function was there-

fore determined between two C_{carb} atoms (Figure SI.2 on Supporting Information). Figure 2 shows the snapshots of box as a function of the DEH*i*BA molar fraction on the mixture (*n*-dodecane + DEH*i*BA), only DEH*i*BA molecules are represented. The Figures SI.4, SI.5 and SI.6 on Supporting Information shows the radial distribution functions (RDF) between two C_{carb} carbon atoms of the extractant molecules for different extractants molar fraction respectively for the mixtures (*n*-dodecane + DEH*i*BA), (*n*-dodecane + DEHBA) and (*n*-heptane + DEH*i*BA). The absence of aggregation is consistent with previous experimental studies with the system (DEH*i*BA-*n*-heptane) [72]. For mixtures containing DEH*i*BA, a first insignificant peak can be seen at about 4 Å and a second peak at about 6 Å. For the mixture containing DEHBA, there is a first significant peak at 6 Å. In any case, the increase in the molar fraction does not significantly increase the coordination between the extracting molecules and the distance from the first peak of $g(r_{C_{\mathrm{carb}}-C_{\mathrm{carb}}})$. From this, we can conclude that no aggregate of extractant molecules is formed. This does not exclude a probable clustering of the mixture in which local densities are different from macroscopic density but globally aggregation is weak.

4.3. Decomposition of contributions

Previously, we presented a method to determine excess enthalpies, either by experiment from the enthalpy of dilution or by molecular dynamics simulations from the enthalpy of the mixture. We were also able to determine the order of magnitude of the excess enthalpies of our mixtures. Figure 9 shows the excess enthalpy as a function of the mole fraction of monoamide, for the (*n*-dodecane+DEH*i*BA) mixture (red line), for the (*n*-dodecane+DEHBA) mixture (green line) and for the (*n*-heptane+DEH*i*BA) mixture (blue line). It is therefore possible to classify these mixtures in ascending order (*n*-heptane+DEH*i*BA) > (*n*-dodecane+DEH*i*BA) > (*n*-dodecane+DEH*i*BA). In this section, we present an energetic decomposition of the excess enthalpy.

The properties of a molecule are deduced by adding the properties of the different functional groups that compose it, this is the concept of group con-

tributions. In the same way, for binary mixtures (n-alkane/monoamides), it is possible to decompose the contributions related to the interaction between the different species that make it up: monoamide/monoamide, n-alkane/n-alkane and n-alkane/monoamide. In practice, the monoamide/monoamide and n-alkane/n-alkane interactions are easily accessible and the n-alkane/monoamide interaction will be deduced by calculation. To do this, the interaction between the monoamides molecules is determined by simulating removing the n-alkane molecules from the system and the interaction between the n-alkane molecules is determined by removing the monoamide molecules from the system for each mole fraction ($0.1 < x < 0.9$), so the coordinates of the molecules in these new configurations are the same as those in the mixture. The behaviour of these configurations is simulated for a single simulation step (1000 fs) and this allows us to calculate the molar enthalpy between monoamides molecules, $h_{\mathrm{MM}}(x)$, and the molar enthalpy between n-alkanes molecules, $h_{\mathrm{AA}}(x)$. The term of cross interaction between monoamides and n-alkanes molecules, $h_{\mathrm{AM}}(x)$, is obtained by the difference between the total enthalpy and the enthalpies $h_{\mathrm{MM}}(x)$ and $h_{\mathrm{AA}}(x)$:

$$h_{\mathrm{AM}}(x) = h(x) - h_{\mathrm{MM}}(x) - h_{\mathrm{AA}}(x) \tag{30}$$

In practice, the enthalpy of excess $h^{\mathrm{E}}(x)$ has already been determined previously. To determine $h^{\mathrm{E}}_{\mathrm{MM}}(x)$ and $h^{\mathrm{E}}_{\mathrm{AA}}(x)$ the enthalpies $h_{\mathrm{MM}}(x)$ and $h_{\mathrm{AA}}(x)$ are adjusted in the same way as for the enthalpy of the mixture (Eq. 19) and for the same polynomial order n ($n = 1$ for mixtures with n-dodecane and $n = 2$ for mixtures with n-heptane). Finally, the excess enthalpy of the cross term is calculated by :

$$h^{\mathrm{E}}_{\mathrm{AM}}(x) = h^{\mathrm{E}}(x) - h^{\mathrm{E}}_{\mathrm{MM}}(x) - h^{\mathrm{E}}_{\mathrm{AA}}(x) \tag{31}$$

The energy decomposition representing the different enthalpies of excess for the system (n-dodecane + DEHiBA), (n-dodecane + DEHBA) and(n-heptane + DEHiBA) is shown in Figure 10.

Negative contributions are favourable and positive contributions are unfavourable. It is important to note here, that the mixture (n-heptane + DE-

HBA) has not been studied. But the comparison of the other mixtures showed that the higher (and positive) the enthalpy of excess, the more alkane has a long chain length and monoamide has isobutyl branching. This excess enthalpy can therefore be classified : (n-dodecane + DEHiBA) > (n-dodecane + DEHBA) > (n-heptane + DEHiBA).

The n-alkane/n-alkane contributions are > 0 (n-dodecane + DEHiBA < $n$dodecane + DEHBA < n-heptane + DEHiBA). Bothorel et *al.* assumed that mixtures containing short-chain n-alkanes (n-heptane) had a lower molecular orientation compared to mixtures containing long-chain n-alkanes (n-dodecane) [56]. In the mixtures, n-alkane molecules have a different molecular orientation than molecules in pure systems. Since this contribution is more unfavourable the shorter the chain length of the n-alkane (and the butyl-branched monoamide), it is possible to link a less favourable contribution to a mixture containing a long-chain n-alkane.

The monoamide/monoamide contributions are < 0 (n-dodecane + DEHiBA > n-dodecane + DEHBA > n-heptane + DEHiBA). Schwabe *et al.* has qualitatively investigated the excess enthalpy of (n-hexane+TiBP) and (n-hexane+TiBP) systems [53]. The conclusion of this work is that the enthalpy of excess is higher in favour of the mixture containing isobutyl branching. The same type of behaviour has been reported with other molecules [54, 55] and is thought to be due to the capacity of molecules containing isobutyl branching to disorder molecularly oriented n-alkane molecules more efficiently. Since this contribution is more favourable when the chain length is short and the monoamide has a butyl branch, it is possible to link a less favourable contribution to a mixture containing a long-chain n-alkane and an isobutyl-branched monoamide.

The n-alkane/monoamide contribution are > 0 (n-dodecane + DEHiBA > n-dodecane + DEHBA > n-heptane + DEHiBA). They are more unfavourable the more the chain length of the n-alkane increases and the more the monoamide has isobutyl branching. This corroborates the previous observations: mixtures containing long-chain n-alkanes and monoamides with isobutyl branching show a greater deviation from ideality than mixtures containing short-chain n-alkanes,

which are more ideal.

Globally, the total excess enthalpies are such that these mixtures are energetically not very different from simple regular solutions. Nevertheless, the detailed balance between the two species plotted in Figure 10 leads to different conclusions. There is no symmetry between the two components. In any case, an important attraction between the extractants is obtained since the corresponding mixing enthalpy is negative. This can lead to the formation of macromolecular entities favouring extraction.

5. Conclusion

We experimentally measured by ITC and calculated from molecular dynamics simulations at a temperature of 298.15 K and a pressure of 1 bar, the enthalpy of the mixture, the dilution enthalpy and excess enthalpy for the systems (n-alkanes+N,N-dialkylamides). The experimental study of the system (n-dodecane + DEHiBA) presented the method for determining the excess enthalpy from the dilution enthalpy. The enthalpy of the experimental mixture could be estimated using the enthalpy of experimental excess and the enthalpies of pure compound calculated by molecular dynamics. We then calculated the enthalpy of excess of the mixture (n-dodecane + DEHBA) and compared it to that of the mixture (n-dodecane + DEHiBA). We determined that the enthalpy of excess was higher in favour of the mixture containing the extracting molecule with isobutyl branching.

For these extractant molecules diluted in n-dodecane, the excess enthalpy is about 423 J mol^{-1} higher in favour of mixing with the isobutyl branching (DEHiBA). We found this behaviour in mixtures of type (haloalkanes + n-alkanes) [54, 55] and (phosphorus extractant + n-alkane) [37, 36, 53]. Indeed, the enthalpy of excess of the systems (terbutylchloride + n-alkane) is always higher than that of the systems (1-chlorobutane+n-alkane) and that of the system (TiBP + n-hexane) is always higher than the system (TBP + n-hexane). The study of radial distribution functions has shown that N,N-dialkylamide

molecules do not self-associate as is the case with neutral organophosphorus extractant molecules [36, 38]. The endothermicity of the mixture (*n*-dodecane + DEH*i*BA) would therefore be due only to physical interaction between the molecules. With the comparison of this two binary systems, it would seems that the asymmetry of the excess enthalpy is due to a significant difference between the molar volumes of the components of the mixture as reported by Fenby [58]. Nevertheless this asymmetry is weak and the mixtures are not very different from regular solutions. The study of the system (*n*-heptane + DEH*i*BA) allowed to see the influence of the force field on the calculated thermodynamic quantities. A necessary condition for a good estimation of the enthalpies of excess, dilution and the mixture is to have a very accurate force field allowing a good evaluation of the energy properties of the pure compounds.

Globally the methodology presented here confirms that the force-field is able to describe accurately mixing enthalpies in these systems. As already mentioned, this is an important test because enthalpy is directly related to the simulated force-field. The methodology we proposed here can be applied to any mixture for which such experiments are possible. Thus, calorimetry appears to be a method of choice for linking experiments and molecular modelling in these complex liquid mixtures, and experimental developments could benefit from using it more often. Calorimetry is thus probably one of the first methods to be used to couple simulations and experiments since it allows direct validation of the force field.

Nevertheless, if the interest of enthalpy comes from the fact that it is a direct average of the interactions on the molecular configurations, this also constitutes its limits because the method does not give direct information on the organization of the system. For example, if the enthalpy variations seem to simply reflect mixing rules similar to regular solutions, this does not mean that a certain aggregation does not take place. This entropic phenomenon in fact only marginally changes the enthalpy, by modifying the neighbourhood of each molecule. The full study of the phenomena present in the extraction therefore requires in any case to take into account these organisational phenomena,

especially in the presence of metal ions. In this case, the coupling between simulation and experiment could implement other techniques more sensitive to the structure of the medium.

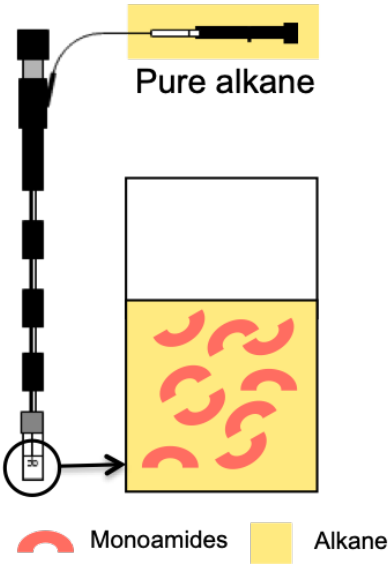

Figure 1: Schematic diagram of microcalorimetric dilution

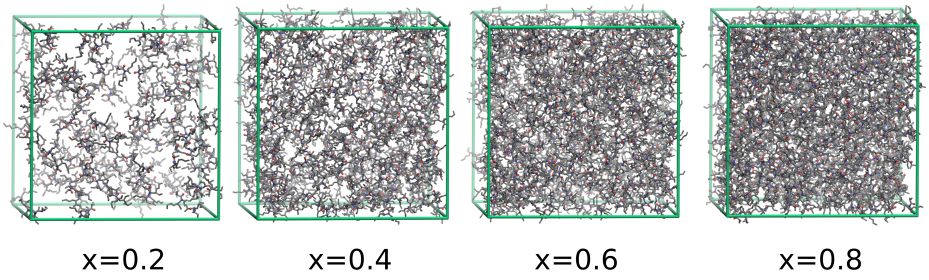

Figure 2: Snapshots of DEH*i*BA molecules in binary mixtures with *n*-dodecane for different DEH*i*BA molar fraction (*n*-dodecane molecules are not represented).

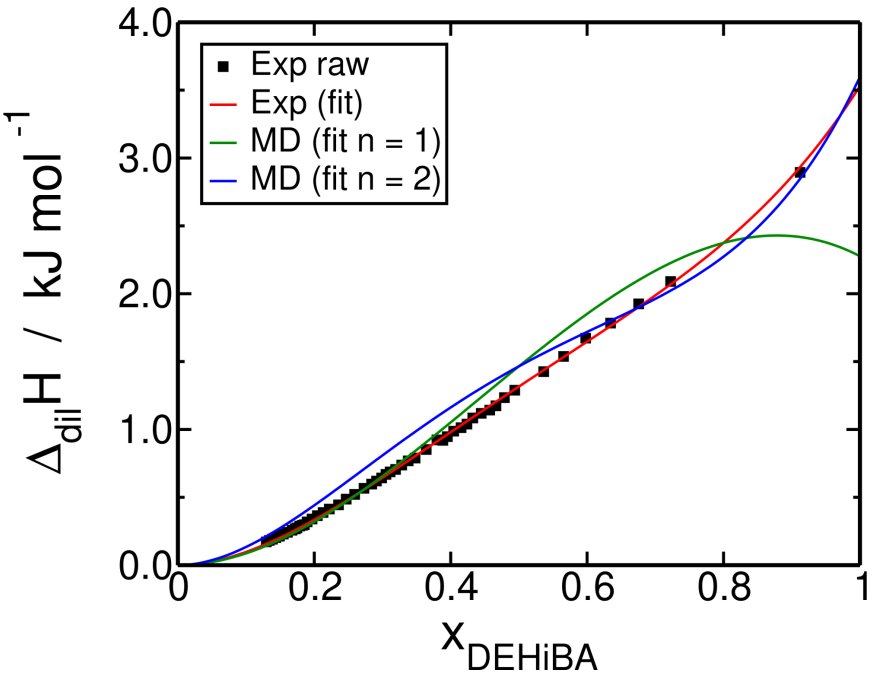

Figure 3: Dilution enthalpy as a function of the molar fraction of DEH*i*BA for the *n*-dodecane+DEH*i*BA mixture obtained experimentally (black square), fitted from the raw experimental data using $n = 2$ in Equation 20 (red line) and fitted from the raw molecular dynamics simulations data using $n = 1$ (green line) and $n = 2$ (blue line) in Equation 20

.

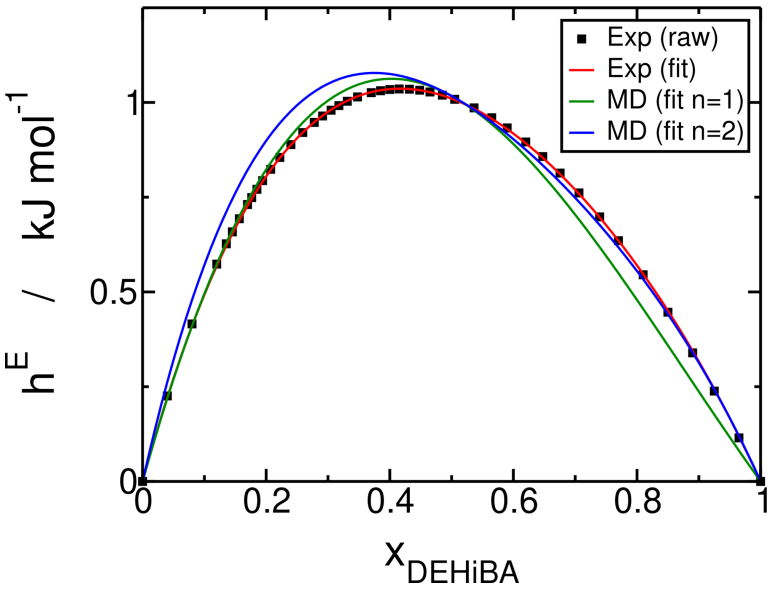

Figure 4: Excess enthalpy as a function of the molar fraction of DEH*i*BA for the (*n*-dodecane+DEH*i*BA) mixture obtained by integration of the raw experimental data (black squares), fitted from the raw experimental data using the Redlich-Kister model with $n = 2$ (red line), and fitted from the raw molar enthalpy $h(x)$ calculated by molecular dynamics using the Redlich-Kister model with $n = 1$ (green line) and $n = 2$ (blue line) (Eq. 18).

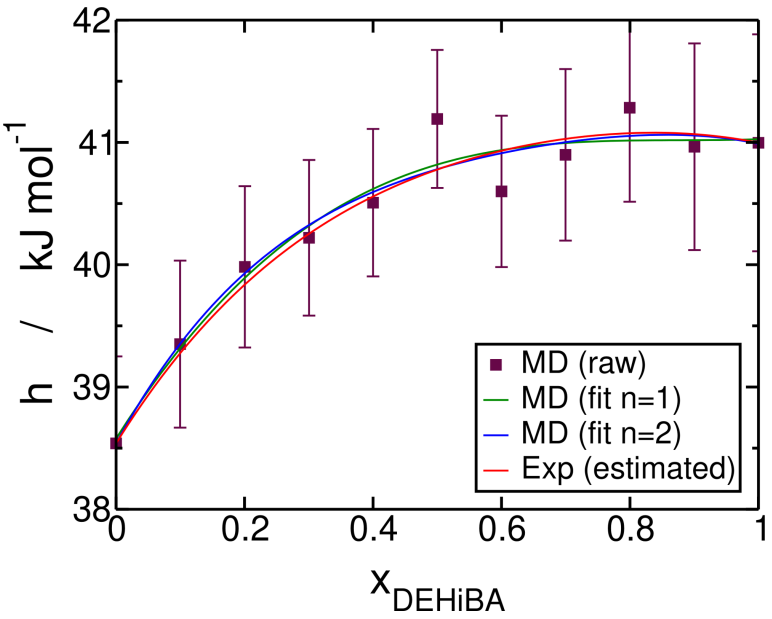

Figure 5: Molar enthalpy as a function of the molar fraction of DEH*i*BA for the *n*-dodecane+DEH*i*BA mixture calculated from the molecular dynamics raw data (brown squares), obtained by fitting Equation 3 with $n = 1$ (green line) and $n = 2$ (blue line), and obtained experimentally (red line) by adding the ideal term calculated by the molar excess enthalpy obtained by adjusting the parameters (red line in Fig. 4)

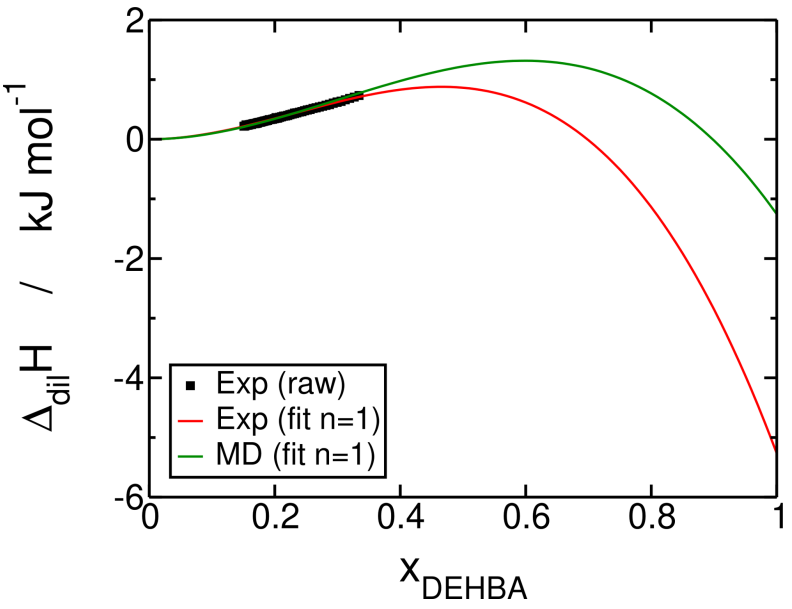

Figure 6: Dilution enthalpy as a function of the molar fraction of DEHBA for the *n*-dodecane+DEHBA mixture obtained experimentally (black squares), fitted from the raw experimental data using $n = 1$ in in Equation 20 (red line), and fitted from the raw molecular dynamics simulations data using $n = 1$ (green line) in Equation 20.

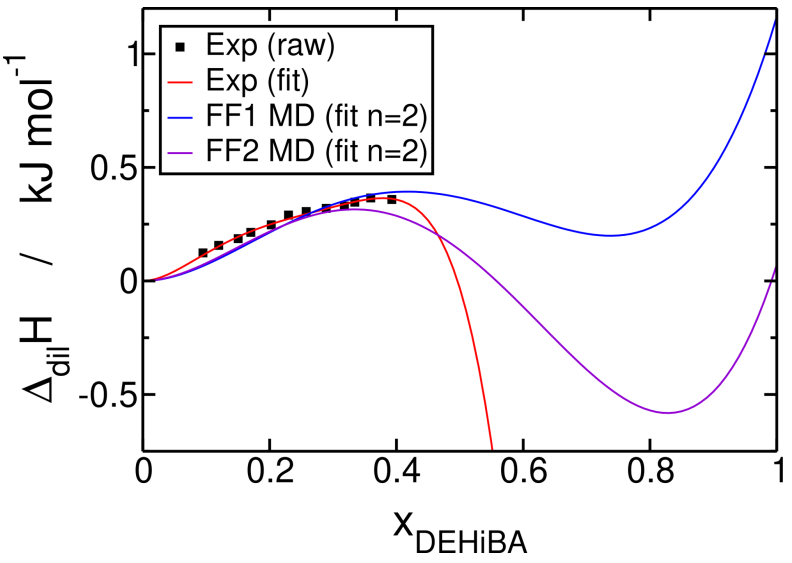

Figure 7: Enthalpy of dilution as a function of the molar fraction of DEH*i*BA for the *n*-heptane+DEH*i*BA mixture obtained experimentally (black square), fitted from the raw molecular dynamics simulations data using $n = 2$ in Equation 20 with the first (blue line) and the second (purple line) force field.

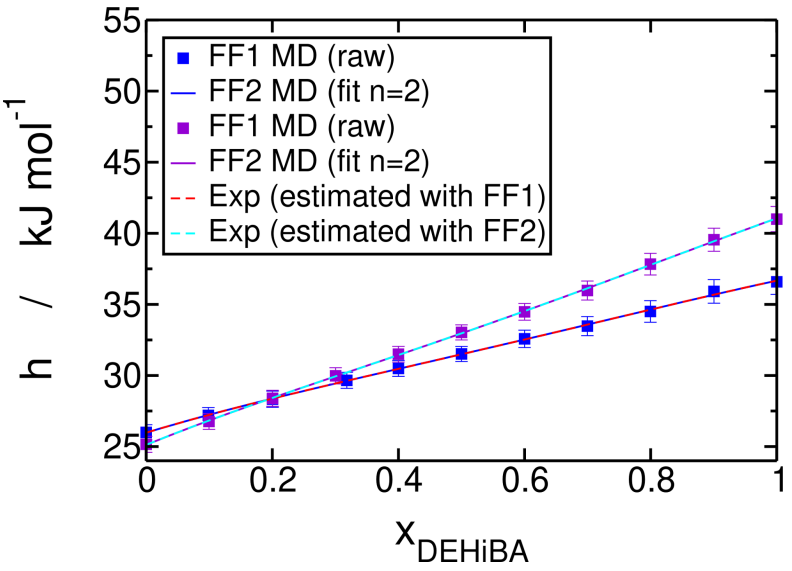

Figure 8: Molar enthalpy as a function of the molar fraction of DEH*i*BA for the (*n*-heptane+DEH*i*BA) mixture calculated from the molecular dynamics raw data (respectively blue and purple squares for the first and the second force field), obtained by fitting Equation 19 with $n = 2$ (respectively blue and purple lines for the first and the second force field) and obtained experimentally (respectively red and cyan dotted lines for the first and the second force field) by adding the ideal term calculated by molecular dynamics simulations to the excess enthalpy obtained by integration.

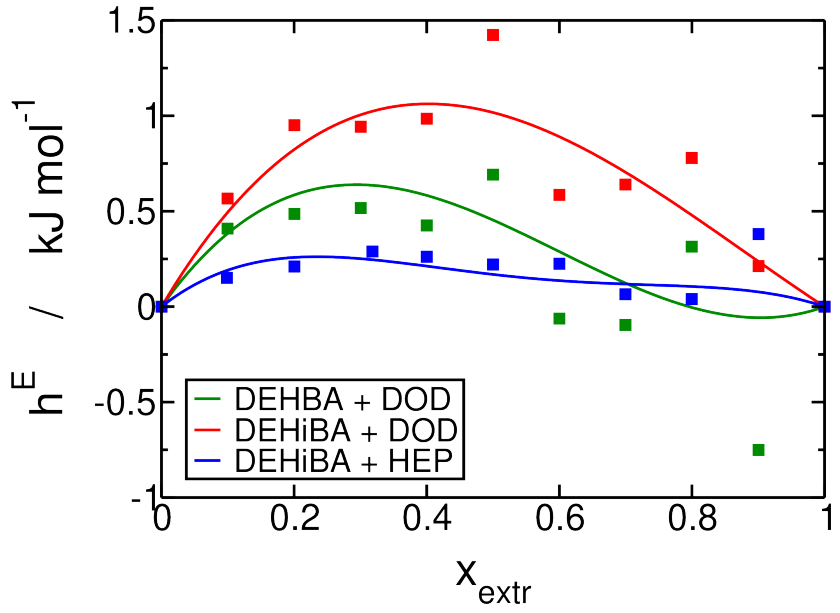

Figure 9: Excess enthalpy as a function of the molar fraction of monoamide for the mixture *n*-dodecane+DEH*i*BA (red line), for the mixture *n*-dodecane+DEHBA (green line) and for the mixture *n*-heptane+DEH*i*BA (blue line), the squares represents the molecular dynamics raw excess enthalpy respectively for the three systems

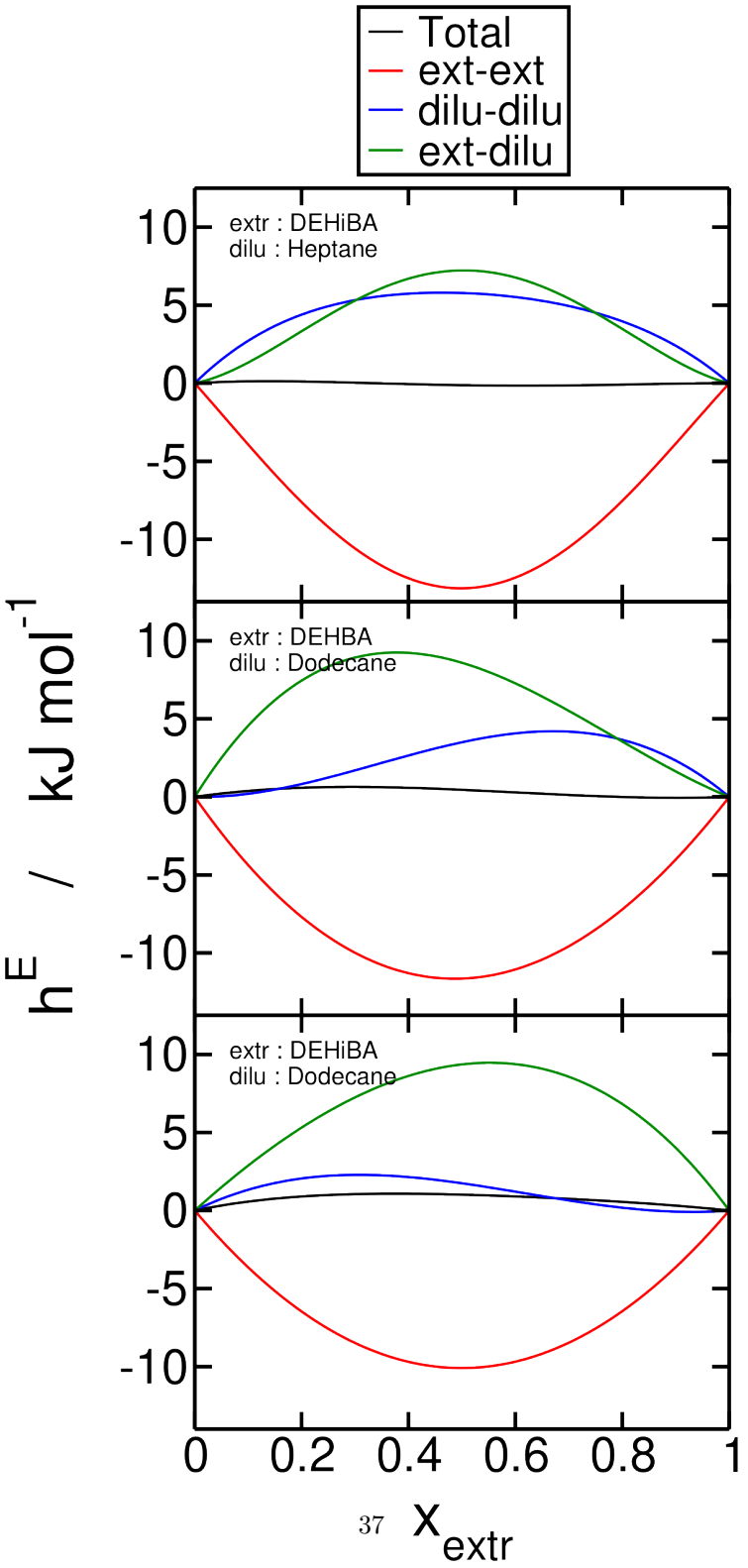

Figure 10: Decomposition of the excess enthalpy

6. Acknowledgments

References

[1] R. C. Ewing, Long-term storage of spent nuclear fuel, Nature Materials 14 (3) (2015) 252–257. doi:10.1038/nmat4226.

[2] J. Bruno, R. C. Ewing, Spent Nuclear Fuel, Elements 2 (6) (2006) 343–349. doi:10.2113/gselements.2.6.343.

[3] C. Marie, M. Miguirditchian, D. Guillaumont, A. Tosseng, C. Berthon, P. Guilbaud, M. Duvail, J. Bisson, D. Guillaneux, M. Pipelier, D. Dubreuil, Complexation of Lanthanides(III), Americium(III), and Uranium(VI) with Bitopic N,O Ligands: an Experimental and Theoretical Study, Inorganic Chemistry 50 (14) (2011) 6557–6566. doi:10.1021/ic200271e.

[4] M.-C. Charbonnel, C. Berthon, L. Berthon, N. Boubals, F. Burdet, M.-T. Duchesne, P. Guilbaud, N. Mabille, S. Petit, N. Zorz, Complexation of Ln(III) and Am(III) with the Hydrosoluble TEDGA: Speciation and Thermodynamics Studies, Procedia Chemistry 7 (2012) 20–26. doi:10.1016/j.proche.2012.10.005.

[5] B. Qiao, T. Demars, M. Olvera de la Cruz, R. J. Ellis, How Hydrogen Bonds Affect the Growth of Reverse Micelles around Coordinating Metal Ions, The Journal of Physical Chemistry Letters 5 (8) (2014) 1440–1444. doi:10.1021/jz500495p.

[6] B. Qiao, J. V. Muntean, M. Olvera de la Cruz, R. J. Ellis, Ion Transport Mechanisms in Liquid–Liquid Interface, Langmuir 33 (24) (2017) 6135–6142. doi:10.1021/acs.langmuir.7b01230.

[7] A. Das, S. M. Ali, Molecular Dynamics Simulation Studies on Structure, Dynamics, and Thermodynamics of Uranyl Nitrate Solution at Various Acid Concentrations, The Journal of Physical Chemistry B 123 (21) (2019) 4571–4586. doi:10.1021/acs.jpcb.9b01498.

[8] B. Qiao, G. Ferru, M. Olvera de la Cruz, R. J. Ellis, Molecular Origins of Mesoscale Ordering in a Metalloamphiphile Phase, ACS Central Science 1 (9) (2015) 493–503. doi:10.1021/acscentsci.5b00306.

[9] F. Rodrigues, G. Ferru, L. Berthon, N. Boubals, P. Guilbaud, C. Sorel, O. Diat, P. Bauduin, J. Simonin, J. Morel, N. Morel-Desrosiers, M. Charbonnel, New insights into the extraction of uranium(VI) by an N,N-dialkylamide, Molecular Physics 112 (9-10) (2014) 1362–1374. doi:10.1080/00268976.2014.902139.

[10] X.-H. Kong, Q.-Y. Wu, X.-R. Zhang, C. Wang, K.-Q. Hu, Z.-F. Chai, C.-M. Nie, W.-Q. Shi, Coordination behavior of uranyl with PDAM derivatives in solution: Combined study with ESI-MS and DFT, Journal of Molecular Liquids 300 (2020) 112287. doi:10.1016/j.molliq.2019.112287.

[11] E. Acher, T. Dumas, C. Tamain, N. Boubals, P. L. Solari, D. Guillaumont, Inner to outer-sphere coordination of plutonium(IV) with N,N-dialkyl amide: influence of nitric acid, Dalton Transactions 46 (12) (2017) 3812–3815. doi:10.1039/C7DT00031F.

[12] E. Acher, Y. Hacene Cherkaski, T. Dumas, C. Tamain, D. Guillaumont, N. Boubals, G. Javierre, C. Hennig, P. L. Solari, M.-C. Charbonnel, Structures of Plutonium(IV) and Uranium(VI) with Dialkyl Amides from Crystallography, X-ray Absorption Spectra, and Theoretical Calculations, Inorganic Chemistry 55 (11) (2016) 5558–5569. doi:10.1021/acs.inorgchem.6b00592.

[13] V. Vallet, U. Wahlgren, B. Schimmelpfennig, H. Moll, Z. Szabó, I. Grenthe, Solvent Effects on Uranium(VI) Fluoride and Hydroxide Complexes Studied by EXAFS and Quantum Chemistry, Inorganic Chemistry 40 (14) (2001) 3516–3525. doi:10.1021/ic001405n.

[14] U. Wahlgren, H. Moll, I. Grenthe, B. Schimmelpfennig, L. Maron, V. Vallet, O. Gropen, Structure of Uranium(VI) in Strong Alkaline Solutions.

A Combined Theoretical and Experimental Investigation, The Journal of Physical Chemistry A 103 (41) (1999) 8257–8264. doi:10.1021/jp990042d.

[15] O. Pecheur, S. Dourdain, D. Guillaumont, J. Rey, P. Guilbaud, L. Berthon, M. Charbonnel, S. Pellet-Rostaing, F. Testard, Synergism in a HDEHP/TOPO Liquid–Liquid Extraction System: An Intrinsic Ligands Property?, The Journal of Physical Chemistry B 120 (10) (2016) 2814–2823. doi:10.1021/acs.jpcb.5b11693.

[16] P. V. Dau, Z. Zhang, Y. Gao, B. F. Parker, P. D. Dau, J. K. Gibson, J. Arnold, M. Tolazzi, A. Melchior, L. Rao, Thermodynamic, Structural, and Computational Investigation on the Complexation between UO_2^{2+} and Amine-Functionalized Diacetamide Ligands in Aqueous Solution, Inorganic Chemistry 57 (4) (2018) 2122–2131. doi:10.1021/acs.inorgchem.7b02971.

[17] J. Mu, R. Motokawa, K. Akutsu, S. Nishitsuji, A. J. Masters, A Novel Microemulsion Phase Transition: Toward the Elucidation of Third-Phase Formation in Spent Nuclear Fuel Reprocessing, The Journal of Physical Chemistry B 122 (4) (2018) 1439–1452. doi:10.1021/acs.jpcb.7b08515.

[18] A. Paquet, O. Diat, L. Berthon, P. Guilbaud, Aggregation in organic phases after solvent extraction of uranyl nitrate: X-ray scattering and molecular dynamic simulations, Journal of Molecular Liquids 277 (2019) 22–35. doi:10.1016/j.molliq.2018.12.051.

[19] P. Distler, K. Stamberg, J. John, L. M. Harwood, F. W. Lewis, Thermodynamic parameters of Am(III), Cm(III) and Eu(III) extraction by CyMe4-BTPhen in cyclohexanone from HNO3 solutions, The Journal of Chemical Thermodynamics 141 (2020) 105955. doi:10.1016/j.jct.2019.105955.

[20] L. Rao, G. Tian, Thermodynamic study of the complexation of uranium(VI) with nitrate at variable temperatures 40 (6) 1001–1006. doi:10.1016/j.jct.2008.02.013.

[21] J. Jiang, J. C. Renshaw, M. J. Sarsfield, F. R. Livens, D. Collison, J. M. Charnock, H. Eccles, Solution Chemistry of Uranyl Ion with Iminodiacetate and Oxydiacetate: A Combined NMR/EXAFS and Potentiometry/Calorimetry Study, Inorganic Chemistry 42 (4) (2003) 1233–1240. doi:10.1021/ic020460o.

[22] A. P. Paiva, P. Malik, Recent advances on the chemistry of solvent extraction applied to the reprocessing of spent nuclear fuels and radioactive wastes, Journal of Radioanalytical and Nuclear Chemistry 261 (2) (2004) 485–496. doi:10.1023/B:JRNC.0000034890.23325.b5.

[23] T. H. Siddall, Effects of structure of n,n-disubstituted amides on their extraction of actinide and zirconium nitrates and of nitric acid, The Journal of Physical Chemistry 64 (12) (1960) 1863–1866. doi:10.1021/j100841a014.

[24] N. Condamines, C. Musikas, The extraction by n,n-dialkylamides. ii. extraction of actinide cations, Solvent Extraction and Ion Exchange 10 (1) (1992) 69–100. doi:10.1080/07366299208918093.

[25] P. Pathak, L. Kumbhare, V. Manchanda, Effect of structure of n,n dialkyl amides on the extraction of U(VI) and Th(IV): a thermodynamic study, Radiochimica Acta 89 (7) (2001) 447–452. doi:10.1524/ract.2001.89.7.447.

[26] D. R. Prabhu, G. R. Mahajan, G. M. Nair, Di(2-ethyl hexyl) butyramide and di(2-ethyl hexyl)isobutyramide as extractants for uranium(VI) and plutonium(IV), Journal of Radioanalytical and Nuclear Chemistry 224 (1-2) (1997) 113–117. doi:10.1007/BF02034622.

[27] P. N. Pathak, D. R. Prabhu, N. Kumari, A. S. Kanekar, V. K. Manchanda, Evaluation of N,N-dihexyloctanamide as an alternative extractant for spent fuel reprocessing: batch and mixer settler studies 38 (2012) 40–45. doi:10.1080/19443994.2012.664262.

[28] K. K. Gupta, V. K. Manchanda, M. S. Subramanian, R. K. Singh, N,N-Dihexyl Hexanamide: A Promising Extractant for Nuclear Fuel Repro-

cessing, Separation Science and Technology 35 (10) (2000) 1603–1617. doi:10.1081/SS-100100243.

[29] P. K. Verma, P. N. Pathak, N. Kumari, B. Sadhu, M. Sundararajan, V. K. Aswal, P. K. Mohapatra, Effect of Successive Alkylation of N,N-Dialkyl Amides on the Complexation Behavior of Uranium and Thorium: Solvent Extraction, Small Angle Neutron Scattering, and Computational Studies, The Journal of Physical Chemistry B 118 (49) (2014) 14388–14396. doi:10.1021/jp5074285.

[30] N. Sieffert, G. Wipff, Uranyl extraction by N,N-dialkylamide ligands studied using static and dynamic DFT simulations, Dalton Transactions 44 (6) (2015) 2623–2638. doi:10.1039/C4DT02443E.

[31] P. Moeyaert, T. Dumas, D. Guillaumont, K. Kvashnina, C. Sorel, M. Miguirditchian, P. Moisy, J.-F. Dufrêche, Modeling and Speciation Study of Uranium(VI) and Technetium(VII) Coextraction with DEHiBA, Inorganic Chemistry 55 (13) (2016) 6511–6519. doi:10.1021/acs.inorgchem.6b00595.

[32] R. Malmbeck, D. Magnusson, S. Bourg, M. Carrott, A. Geist, X. Hérès, M. Miguirditchian, G. Modolo, U. Müllich, C. Sorel, R. Taylor, A. Wilden, Homogenous recycling of transuranium elements from irradiated fast reactor fuel by the EURO-GANEX solvent extraction process, Radiochimica Acta 107 (9-11) (2019) 917–929. doi:10.1515/ract-2018-3089.

[33] K. McCann, B. J. Mincher, N. C. Schmitt, J. C. Braley, Hexavalent Actinide Extraction Using N,N-Dialkyl Amides, Industrial & Engineering Chemistry Research 56 (22) (2017) 6515–6519. doi:10.1021/acs.iecr.7b01181.

[34] Y. Marcus, Z. Kolarik, Thermodynamics of liquid-liquid distribution reactions. I. Dioxouranium(VI) nitrate-water-tributyl phosphate-n-dodecane system, Journal of Chemical & Engineering Data 18 (2) (1973) 155–163. doi:10.1021/je60057a019.

[35] F. Rodrigues, N. Boubals, M.-C. Charbonnel, N. Morel-Desrosiers, Thermodynamic Approach of Uranium(VI) Extraction by N,N-(2–ethylhexyl)Isobutyramide, Procedia Chemistry 7 (2012) 59–65. doi:10.1016/j.proche.2012.10.011.

[36] L. Tsimering, A. S. Kertes, Excess enthalpies of tri-*n*-butylphosphate + hydrocarbons, The Journal of Chemical Thermodynamics 6 (1974) 411–415. doi:10.1016/0021-9614(74)90001-9.

[37] A. S. Kertes, L. Tsimering, Thermodynamics of solvent extraction processes: Heat capacities, heats of mixing and solution of organophosphorus extractants in dodecane, The Journal of Chemical Thermodynamics 39 (4) (1977) 649–651. doi:10.1016/0022-1902(77)80581-2.

[38] M. J. Servis, D. T. Wu, J. C. Shafer, The role of solvent and neutral organophosphorus extractant structure in their organization and association, Journal of Molecular Liquids 253 (2018) 314–325. doi:10.1016/j.molliq.2018.01.031.

[39] A. Wright, P. Paviet-Hartmann, Review of Physical and Chemical Properties of Tributyl Phosphate/Diluent/Nitric Acid Systems, Separation Science and Technology 45 (12-13) (2010) 1753–1762. doi:10.1080/01496395.2010.494087.

[40] X. Ye, S. Cui, V. d. Almeida, B. Khomami, Interfacial Complex Formation in Uranyl Extraction by Tributyl Phosphate in Dodecane Diluent: A Molecular Dynamics Study, The Journal of Physical Chemistry B 113 (29) (2009) 9852–9862. doi:10.1021/jp810796m.

[41] J. Bisson, B. Dinh, P. Huron, C. Huel, PAREX, A Numerical Code in the Service of La Hague Plant Operations, Procedia Chemistry 21 (2016) 117–124. doi:10.1016/j.proche.2016.10.017.

[42] H. Piekarski, Thermochemistry of electrolyte solutions: Effect of added

cosolvent, Journal of Thermal Analysis and Calorimetry 108 (2) (2012) 537–545. doi:10.1007/s10973-011-2019-2.

[43] T. Lazaridis, Inhomogeneous fluid approach to solvation thermodynamics. 1. theory, Journal of Physical Chemistry B 102 (18) (1998) 3531–3541. doi:doi.org/10.1021/jp9723574.

[44] E. Gallicchio, M. M. Kubo, R. M. Levy, Enthalpy-entropy and cavity decomposition of alkane hydration free energies: Numerical results and implications for theories of hydrophobic solvation, Journal of Physical Chemistry B 104 (26) (2000) 6271–6285. doi:doi.org/10.1021/jp0006274.

[45] A. M. Zaichikov, M. A. Krest'yaninov, Thermodynamic parameters of solvation of nonelectrolytes in aqueous solutions with hydrogen bond networks, Russian Journal of General Chemistry 78 (4) (2008) 543–550. doi:10.1134/S1070363208040063.

[46] M. Duvail, T. Dumas, A. Paquet, A. Coste, L. Berthon, P. Guilbaud, UO_2^{2+} structure in solvent extraction phases resolved at molecular and supramolecular scales: a combined molecular dynamics, EXAFS and SWAXS approach, Physical Chemistry Chemical Physics 21 (15) (2019) 7894–7906. doi:10.1039/C8CP07230B.

[47] C. Lucks, A. Rossberg, S. Tsushima, H. Foerstendorf, A. C. Scheinost, G. Bernhard, Aqueous Uranium(VI) Complexes with Acetic and Succinic Acid: Speciation and Structure Revisited, Inorganic Chemistry 51 (22) (2012) 12288–12300. doi:10.1021/ic301565p.

[48] C. Hennig, K. Schmeide, V. Brendler, H. Moll, S. Tsushima, A. C. Scheinost, EXAFS Investigation of U(VI), U(IV), and Th(IV) Sulfato Complexes in Aqueous Solution, Inorganic Chemistry 46 (15) (2007) 5882–5892. doi:10.1021/ic0619759.

[49] A. Grossfield, P. Ren, J. W. Ponder, Ion Solvation Thermodynamics from

Simulation with a Polarizable Force Field, Journal of the American Chemical Society 125 (50) (2003) 15671–15682. doi:10.1021/ja037005r.

[50] C. Berger, C. Marie, D. Guillaumont, C. Tamain, T. Dumas, T. Dirks, N. Boubals, E. Acher, M. Laszczyk, L. Berthon, Coordination Structures of Uranium(VI) and Plutonium(IV) in Organic Solutions with Amide Derivatives, Inorganic Chemistry 59 (3) (2020) 1823–1834. doi:10.1021/acs.inorgchem.9b03024.

[51] E. D. Totchasov, M. Y. Nikiforov, G. A. Al'per, Calculations of the enthalpy of solution of nonelectrolytes in mixed solvents within the framework of molecular association theory, Russian Journal of Physical Chemistry A 83 (1) (2009) 45–49. doi:10.1134/S0036024409010105.

[52] J. A. Gonzalez, J. C. Cobos, Thermodynamics of liquid mixtures containing a very strongly polar compound Part 6. DISQUAC characterization of N,N-dialkylamides, Fluid Phase Equilibria 224 (2004) 169–183. doi:10.1016/j.fluid.2004.02.007.

[53] K. Schwabe, K. Wiesener, Thermodynamische messungen an binären gemischen von tri-iso-butylphosphat mit organischen nichtelektrolyten, Zeitschrift für Elektrochemie 66 (1962) 39–45.

[54] J. Valero, M. Gracia, C. Gutierrez Losa, Excess enthalpies of some (chloroalkane + *n*-alkane) mixtures, The Journal of Chemical Thermodynamics 12 (7) (1980) 621–625. doi:10.1016/0021-9614(80)90083-X.

[55] J. Valero, M. Lopez, M. Gracia, C. Gutiérrez Losa, Excess enthalpies of some (bromoalkane + *n*-alkane) mixtures, The Journal of Chemical Thermodynamics 12 (7) (1980) 627–633. doi:10.1016/0021-9614(80)90084-1.

[56] P. Bothorel, C. Such, C. Clément, Étude des corrélations d'orientation moléculaire par diffusion rayleigh dépolarisée dans les liquides purs et les solutions, J. Chim. Phys. 69 (1972) 1453–1461. doi:10.1051/jcp/1972691453.

[57] F. Grauer, A. S. Kertes, Heats of mixing of tri-n-dodecylamine with n-octane, benzene, or chlorobenzene, Journal of Chemical & Engineering Data 18 (4) (1973) 405–407. doi:10.1021/je60059a032.

[58] D. V. Fenby, R. L. Scott, Heats of mixing of nonelectrolyte solutions. IV. Mixtures of fluorinated benzenes, The Journal of Physical Chemistry 71 (12) (1967) 4103–4110. doi:10.1021/j100871a058.

[59] O. Redlich, A. T. Kister, Algebraic Representation of Thermodynamic Properties and the Classification of Solutions, Industrial & Engineering Chemistry 40 (2) (1948) 345–348. doi:10.1021/ie50458a036.

[60] L.-R. Briggner, I. Wadsö, Test and calibration processes for microcalorimeters, with special reference to heat conduction instruments used with aqueous systems, Journal of Biochemical and Biophysical Methods 22 (2) (1991) 101–118. doi:10.1016/0165-022x(91)90023-p.

[61] D. A. Case, V. Babin, J. T. Berryman, R. M. Betz, Q. Cai, D. S. Cerutti, T. E. C. III, T. A. Darden, R. E. Duke, H. Gohlke, A. W. Goetz, S. Gusarov, N. Homeyer, P. Janowski, J. Kaus, I. Kolossváry, A. Kovalenko, T. S. Lee, S. LeGrand, T. Luchko, R. Luo, B. Madej, K. M. Merz, F. Paesani, D. R. Roe, A. Roitberg, C. Sagui, R. Salomon-Ferrer, G. Seabra, C. L. Simmerling, W. Smith, J. Swails, R. C. Walker, J. Wang, R. M. Wolf, X. Wu, P. Kollman, AMBER 14 University of California, San Francisco (2014) http://ambermd.org/.

[62] H. C. Andersen, Molecular dynamics simulations at constant pressure and/or temperature, The Journal of Chemical Physics 72 (4) (1980) 2384–2393. doi:10.1063/1.439486.

[63] H. J. C. Berendsen, J. P. M. Postma, W. F. van Gunsteren, A. DiNola, J. R. Haak, Molecular dynamics with coupling to an external bath, The Journal of Chemical Physics 81 (8) (1984) 3684–3690. doi:10.1063/1.448118.

[64] T. Darden, D. York, L. Pedersen, Particle mesh ewald: An N log N method for Ewald sums in large systems, The Journal of Chemical Physics 98 (12) (1993) 10089–10092. doi:10.1063/1.464397.

[65] W. Humphrey, A. Dalke, K. Schulten, VMD: Visual molecular dynamics, Journal of Molecular Graphics 14 (1) (1996) 33–38. doi:10.1016/0263-7855(96)00018-5.

[66] L. Martínez, R. Andrade, E. G. Birgin, J. M. Martínez, PACKMOL: A package for building initial configurations for molecular dynamics simulations, Journal of Computational Chemistry 30 (13) (2009) 2157–2164. doi:10.1002/jcc.21224.

[67] T. Sukhbaatar, M. Duvail, T. Dumas, S. Dourdain, G. Arrachart, P. L. Solari, P. Guilbaud, S. Pellet-Rostaing, Probing the existence of uranyl trisulfate structures in the AMEX solvent extraction process, Chemical Communications 55 (53) (2019) 7583–7586. doi:10.1039/C9CC02651G.

[68] S. W. I. Siu, K. Pluhackova, R. A. Böckmann, Optimization of the OPLS-AA Force Field for Long Hydrocarbons, Journal of Chemical Theory and Computation 8 (4) (2012) 1459–1470. doi:10.1021/ct200908r.

[69] T. A. Pascal, D. Schärf, Y. Jung, T. D. Kühne, On the absolute thermodynamics of water from computer simulations: A comparison of first-principles molecular dynamics, reactive and empirical force fields, The Journal of Chemical Physics 137 (24) (2012) 244507. doi:10.1063/1.4771974.

[70] C. Vega, M. M. Conde, C. McBride, J. L. F. Abascal, E. G. Noya, R. Ramirez, L. M. Sesé, Heat capacity of water: A signature of nuclear quantum effects, The Journal of Chemical Physics 132 (4) (2010) 046101. doi:10.1063/1.3298879.

[71] Y. Chen, M. Duvail, P. Guilbaud, J.-F. Dufrêche, Stability of reverse micelles in rare-earth separation: a chemical model based on a molecular

approach, Physical Chemistry Chemical Physics 19 (10) (2017) 7094–7100. doi:10.1039/C6CP07843E.

[72] G. Ferru, L. Berthon, C. Sorel, O. Diat, P. Bauduin, J.-P. Simonin, Influence of Extracted Solute on the Organization of a Monoamide Organic Solution, Procedia Chemistry 7 (2012) 27–32. doi:10.1016/j.proche.2012.10.006.